nature astronomy

LETTERS

https://doi.org/10.1038/s41550-020-1123-2

Check for updates

Detection of green line emission in the dayside atmosphere of Mars from NOMAD-TGO observations

J.-C. Gérard[1]✉, S. Aoki[1,2], Y. Willame[2], L. Gkouvelis[1], C. Depiesse[2], I. R. Thomas[2], B. Ristic[2], A. C. Vandaele[2], F. Daerden[2], B. Hubert[1], J. Mason[3], M. R. Patel[3], J.-J. López-Moreno[4], G. Bellucci[5], M. A. López-Valverde[4] and B. Beeckman[3]

The oxygen emission at 557.7 nm is a ubiquitous component of the spectrum of the terrestrial polar aurora and the reason for its usual green colour[1]. It is also observed as a thin layer of glow surrounding the Earth near 90 km altitude in the dayside atmosphere[2,3] but it has so far eluded detection in other planets. Here we report dayglow observations of the green line outside the Earth. They have been performed with the Nadir and Occultation for Mars Discovery ultraviolet and visible spectrometer instrument on board the European Space Agency's ExoMars Trace Gas Orbiter. Using a special observation mode, scans of the dayside limb provide the altitude distribution of the intensity of the 557.7 nm line and its variability. Two intensity peaks are observed near 80 and 120 km altitude, corresponding to photodissociation of CO_2 by solar Lyman α and extreme ultraviolet radiation, respectively. A weaker emission, originating from the same upper level of the oxygen atom, is observed in the near ultraviolet at 297.2 nm. These simultaneous measurements of both oxygen lines make it possible to directly derive a ratio of 16.5 between the visible and ultraviolet emissions, and thereby clarify a controversy between discordant ab initio calculations and atmospheric measurements that has persisted despite multiple efforts. This ratio is considered a standard for measurements connecting the ultraviolet and visible spectral regions. This result has consequences for the study of auroral and airglow processes and for spectral calibration.

The presence of the Martian green line dayglow emission was predicted about 40 years ago[4]. However, observations dedicated to the Martian dayglow have so far been sensitive to radiation beyond 340 nm, and thus focused on the ultraviolet (UV) spectrum[5–8], including the O I 297.2 nm emission. The [O I] 557.7 and 297.2 nm forbidden emissions have the same ^{1}S upper state, so their intensity ratio is equal to that of their transition probability. The two transition probabilities and their ratio $R = I(557.7\,\text{nm})/I(297.2\,\text{nm})$ have been obtained from ab initio calculations. The value recommended by NIST[1] is $R = 16.7$. However, atmospheric observations of the two emissions have led to lower values: $R = 9.8 \pm 1.0$ in the terrestrial nightglow[9] and 9.3 ± 0.5 in the aurora[10]. These values depend on the instrumental calibration of two spectral windows bridged with the O_2 Herzberg I transition. As this ratio is invariant at low pressure, it is a useful standard for measurements connecting the UV and the visible regions.

A new opportunity to explore the visible Martian dayglow was provided by the NOMAD-UVIS instrument on board the Trace Gas Orbiter (TGO). The TGO spacecraft has been orbiting Mars since October 2016 on a circular orbit at ~400 km altitude inclined 74° to the planetary equator. The Nadir and Occultation for Mars Discovery (NOMAD)[11] suite of instruments includes the UV and visible spectrometer (UVIS)[12,13], an ultralight instrument covering the 200–650 nm spectral range that can observe in the nadir and solar occultation modes. It has recently been operated in a special limb mode to collect spectra at the dayside limb. The characteristics of UVIS are summarized in the Methods. As no airglow signal could be observed in the (limb) occultation channel, it was proposed[14] that the TGO spacecraft should be tilted to orient the line of sight of the nadir channel in the limb direction. This procedure was implemented as a test in April 2019.

A total of 24 dayside orbital segments have been analysed so far, corresponding to 48 altitude scans in the limb mode. In the inertial pointing mode used for these measurements, the line of sight of the instrument was fixed in inertial space and scanned altitudes between about 20 and 400 km twice during each orbit as a consequence of the orbital motion. The observations reported here were made during the period between 24 April and 1 December 2019. The Mars solar longitude (L_s) varied between 16° and 115°, from near northern spring equinox to past summer solstice. During this period, the distance of Mars from the Sun varied from 1.59 au to 1.67 au (aphelion). In this observing mode, the altitude resolution at the tangent point depends on the altitude of the spacecraft, the field of view of the instrument and the integration time. The spectra used in this study were integrated over 15 s. The combination of these factors yields a vertical resolution of 10 ± 5 km. The data processing procedure is described in the Methods. From the 24 analysed orbits, two were collected at high solar zenith angles and did not show any measurable green line signal above the 1σ background level. All other orbits exhibit a clear signature at 557.7 nm.

As an example, Fig. 1 shows the average of nine spectra collected between 70 and 100 km altitude during the ingress on 28 April 2019 ($L_s = 18°$). The main spectral feature observed is the [O I] 557.7 nm emission, which is clear above the background level. The intensity distribution around 557.7 nm is fully consistent with the instrumental point spread function and the spectral sampling. The [O I] 297.2 nm emission and the CO_2^+ doublet at 288–289 nm and the

[1]LPAP, STAR Institute, Université de Liège, Liège, Belgium. [2]Royal Belgian Institute for Space Aeronomy, Brussels, Belgium. [3]School of Physical Sciences, The Open University, Milton Keynes, UK. [4]Instituto de Astrofisica de Andalucía/CSIC, Granada, Spain. [5]Istituto di Astrofisica e Planetologia Spaziali, INAF, Rome, Italy. ✉e-mail: jc.gerard@uliege.be

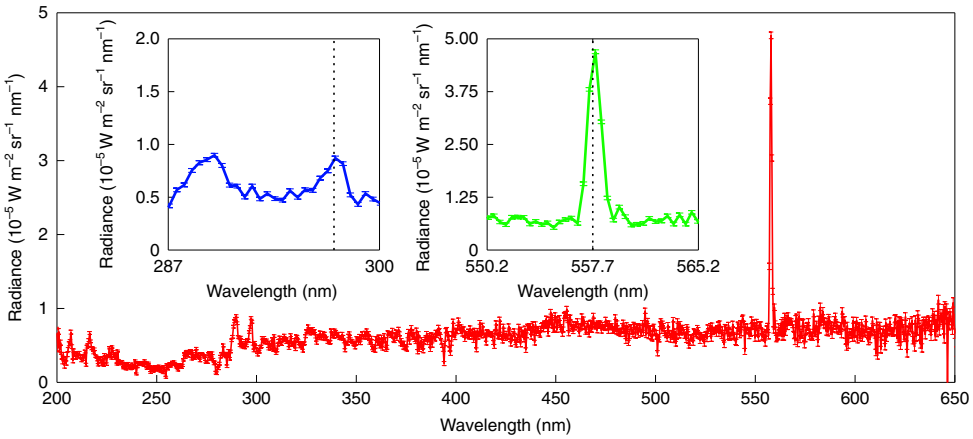

Fig. 1 | Example of UVIS dayside limb spectrum. This averaged spectrum was observed on 28 April 2019 between 70 and 100 km altitude. The insets show the two spectral regions of the CO_2^+ UV doublet and the [OI] 297.2nm emissions (left) and the [OI] 557.7nm (right) green line (vertical dotted lines). L_s was 18°, the latitude of the 80 km tangent point was 10° S and the solar zenith angle was 28°. The signal above 300 nm is a combination of solar scattered light and dayglow emission from the CO_2^+ Fox–Duffendack–Barker bands. The error bars denote the statistical errors in the radiance of individual spectral elements.

long-wavelength tail of the CO Cameron bands are also present as weaker features. In this case, the 557.7 nm peak intensity at 76 km altitude integrated over the line spread function is 245 kR (1 kR corresponds to a surface brightness of 10^9 photons cm^{-2} s^{-1} emitted in 4π steradians).

The evolution of the dayglow spectrum between 70 and 160 km altitude binned over 10 km for the same limb scan as Fig. 1 is illustrated in Fig. 2. It confirms the persistent presence of the [OI] 557.7 nm, [OI] 297.2 nm and CO_2^+ UV doublet emissions observed with IUVS-MAVEN[15,16]. The intensity of the two oxygen lines steadily decreases in parallel above 90 km altitude. In contrast, the brightness of the CO_2^+ doublet peaks near 120 km altitude and becomes barely visible at 160 km altitude in agreement with the IUVS-MAVEN observations. The peak brightness of the UV doublet intensity reaches 57 kR at 118 km altitude, in full agreement with typical intensities and altitudes observed by MAVEN during this season.

The altitude distribution of the 557.7 nm brightness is best illustrated in Fig. 3a, which shows the intensity distribution at the limb collected during the TGO ingress on 28 April 2019. The latitude varied between 25° S at 180 km altitude and 6° S at 60 km altitude, with the local time between 9:45 and 10:26. The brightness of the lower peak has been normalized to unity in Fig. 3b so that the shape of the vertical distribution is clear. A second, weaker peak is also seen near 130 km altitude with an intensity about half of the primary maximum. A similar altitude variation is observed for the weaker 297.2 nm emission (Fig. 3c), with a peak brightness of 14 kR at 80 km. This emission is not absorbed by Martian constituents in the altitude range of the observations. Below 70 km altitude, scattered solar light rapidly exceeds the airglow contribution and makes the intensity estimates uncertain. The upper peak in the distribution is mainly produced by dissociation of CO_2 by solar extreme UV (EUV) radiation leaving a fraction of the O atoms in the ^{1}S state. The lower peak results from the deeper penetration of the solar Lyman α radiation caused by the reduced value of the CO_2 absorption cross-section at 121.6 nm (refs. [4,15,17]). Its altitude is a proxy of the location of the 0.39 μbar level, if the small variation of the gravity in the mesosphere is neglected and a constant mean molecular mass in the overhead atmospheric column is assumed. Monitoring of the changes of the lower emission peak makes it a powerful tool for remotely identifying altitude variations of the pressure level in the mesosphere with latitude, season and atmospheric dust load[15,18].

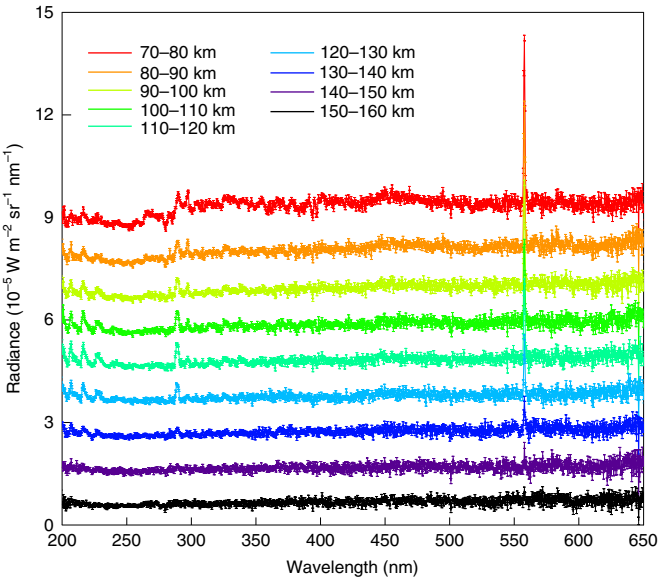

Fig. 2 | Evolution with altitude of the tangent point of the UVIS dayglow spectra observed during the ingress of the same TGO orbit as Fig. 1. The origin of the *y* axis at each altitude below 150 km has been offset by 1×10^{-2} mW m^{-2} sr^{-1} nm^{-1} to improve visibility. The error bars denote the statistical errors in radiance of individual spectral elements.

The absence of the O(^{1}D → ^{3}P) 630–636 nm red doublet (a major component of the terrestrial airglow and aurora) in the UVIS spectra (at the 1σ level) is also notable. Model predictions have indicated that the total production rate of O(^{1}D) atoms exceeds that of O(^{1}S) atoms by nearly an order of magnitude[4]. However, they predicted an intensity ratio I(630 nm)/I(557.7 nm) of as low as 0.01, a consequence of the long radiative lifetime (110 s) of O(^{1}D) and its more efficient collisional deactivation. The lack of any detectable signal at 630 nm is thus consistent with the conclusions of that study.

A comparison of the UVIS 297.2 nm observations with those from IUVS-MAVEN[15,18] provides indirect further confirmation of the detection of the green line. Simultaneous and co-located observations from MAVEN were not possible as the periapsis of MAVEN was on the nightside during the period of the TGO limb observations.

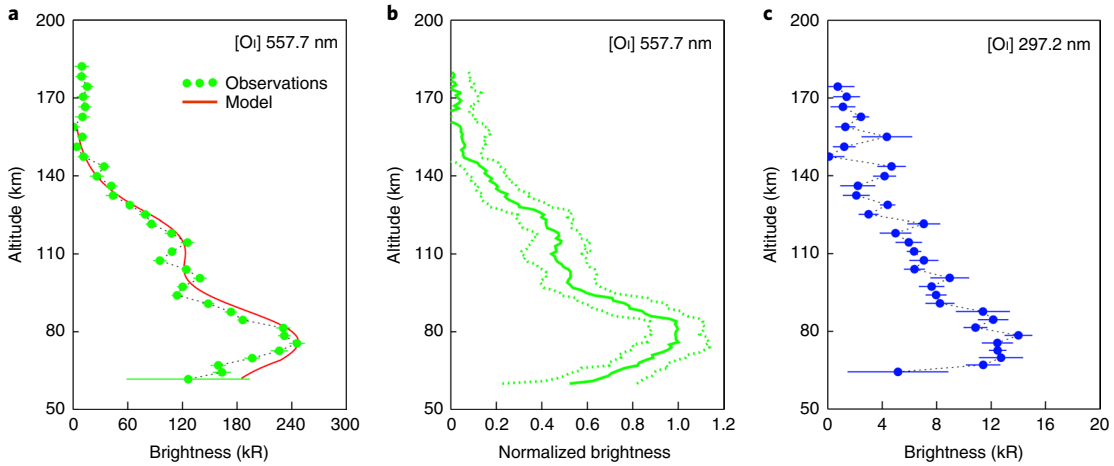

Fig. 3 | Limb profiles observed on 28 April 2019. a, The [OI] 557.7 nm dayglow intensity measured with UVIS on 28 April 2019 (green dots). The green dotted line connects the individual measurements. The red line shows model simulations of the same conditions. The horizontal bars indicate the 1σ uncertainty of the intensity. **b**, The 557.7 nm limb profile (solid line) averaged over 16 limb scans using a 5 km running mean. The dotted line shows the 1σ variability within each bin. **c**, The [OI] 297.2 nm emission observed at the same time as in **a**. The dotted line connects the individual measurements.

However, statistical analysis of IUVS limb scans made at similar solar longitudes show a main peak mean altitude at 77 ± 2 km and a peak intensity of 18 ± 2 kR, in reasonably good agreement with the UVIS limb profile in Fig. 3c with a peak value of 14 kR at 80 km altitude. Consequently, the unambiguous detection of the green line emission in the Martian dayglow is fully confirmed by the absolute brightness and the resemblance between the observed limb profiles and the IUVS observations of the 297.2 nm dayglow. This identification is further demonstrated by the comparison shown in Fig. 3a between the observations and simulations for similar conditions based on a photochemical model[9]. The calculations use neutral atmospheric densities and temperature profiles from the Mars Climate Database (MCD)[19,20] and known sources of O(^{1}S) atoms. The MCD CO_2 density has been scaled down by a factor of 0.5 (ref. [18]). The solar flux is provided by the synthetic spectra with a 1 nm resolution normalized to the three-channel measurements of the EUV monitor (EUVM) on board MAVEN[21]. Future UVIS dayglow observations collected at different seasons, latitudes and local times will make it possible to characterize the CO_2 density variations in the mesosphere, a region otherwise not accessible by in situ measurements.

The mean I(557.7 nm)/I(297.2 nm) ratio is determined from the intensities of the two lines measured in the UVIS spectra in the vicinity of the main emission peak. On the basis of a total of $N = 104$ measurements collected over 16 limb scans, the weighted mean ratio μ is 16.5 ± 0.4, where 0.4 is the standard error on the weighted mean SEM $= \sqrt{\sum_{i=1}^{N} \frac{W_i \times (x_i - \mu)^2}{(N-1) \times \sum_{i=1}^{N} W_i}}$, where W_i are the weights of the N individual ratio values x_i. This intensity ratio is remarkably close to the value of 16.7 recommended by NIST and the relativistic ab initio calculation[22] of 15.5, but not consistent with indirect terrestrial airglow determinations that are substantially lower. This result has consequences for future studies of auroral and airglow processes and for spectral calibration. The discordant values from the terrestrial observations were probably the consequence of the lack of Earth observations with a single calibrated instrument. We recommend that this value be used in planetary and cometary research, as well as laboratory calibration procedures.

Methods

The UVIS spectrometer. The UVIS instrument is composed of two telescopes corresponding to the two geometries of observation. The light from the Sun or the nadir direction is sent through optic fibres to a plane grating and a collimating mirror on the 1,024 × 256 pixel CCD detector. The light is fed to the spectrometer through a single fibre in solar occultation observations or a bundle of optic fibre cables when performing nadir or limb observations. The circular field of view is 2 arcmin for solar occultations and 43 arcmin for the nadir/limb observations. The spectral resolution varies from 1.2 nm at 200 nm to 1.6 nm at 650 nm. The full spectrum is always observed and the only tunable parameters are the integration time (from 0.2 s to a nominal value of 15 s), the spectral binning of the CCD rows and the range of the spectrum sent via the telemetry. Although they use a common detector, the nadir channel is several orders of magnitude more sensitive than the solar occultation channel.

Processing of UVIS spectra and noise removal. The calibration of the UVIS data is performed routinely following several steps. The first step is the removal of the instrumental background or dark current on the CCD frame. The dark current is estimated for each measurement using an interpolation between two 'dark' measurements (that is, measurements recorded with the shutter in front of the slit entrance to work without illumination) taken at the beginning and end of each UVIS orbit. The dark current varies linearly with the integration time and exponentially with the temperature of the CCD. The temperature of the CCD is recorded for each measurement, but must be interpolated across a complete orbit as the temperature discretization is 0.4 °C. The second step is the noise correction, which consists of identifying the cosmic ray detections and the remaining anomalous or hot pixels in the CCD frame that have not been well corrected by the dark current removal. A real signal must appear in all lines of the illuminated region of the CCD to be counted, whereas noisy pixels only appear randomly on the CCD frame. We therefore use a routine that compares the CCD lines to identify the noisy pixels to be excluded. An example of noise removal that confirms the detection of the [OI] 557.7 nm green line and the [OI] 297.2 nm emissions is illustrated in the Supplementary Information. Binning of the CCD lines is then performed, excluding all 'bad' pixels from the noise removal. In the present case, the binning is performed using the 81 fully illuminated CCD lines to increase the signal-to-noise ratio of the observation.

The calibration procedure ends with the conversion of the count rate to units of radiance (W m^{-2} nm^{-1} sr^{-1}) or brightness (kR). The conversion is calculated from laboratory measurements obtained during the calibration campaign. Two lamps with known radiometric response were used to cover the full UVIS spectral range and obtain a count–radiance conversion. Note that solarization of the instrument had been performed previously to slow down ageing of the detector and loss of sensitivity in orbit.

Limb measurements at high altitude are not illuminated and do not require any stray light correction. This is different from standard operation modes (dayside nadir or solar occultation), for which the incoming radiation is important. The critical step here is the noise removal, where the noisy pixel values can reach several orders of magnitude larger than the faint dayglow signal. In addition to the statistical error on the mean ratio given before, a possible systematic error is associated with the uncertainties of the relative instrumental calibration. These uncertainties are estimated to be less than 10%.

Data availability

The data that support the plots within this paper and other findings of this study are available from the BIRA-IASB repository at https://repository.aeronomie.be/?doi=10.18758/71021055 or from the corresponding author on reasonable request.

Received: 27 January 2020; Accepted: 4 May 2020;
Published online: 15 June 2020

References

1. Kramida, A., Ralchenko, Y., Reader, J. & NIST ASD Team *NIST Atomic Spectra Database* version 5.7.1 (NIST, 2019); https://physics.nist.gov/asd
2. Zhang, S. P. & Shepherd, G. G. On the response of the O(^{1}S) dayglow emission rate to the Sun's energy input: an empirical model deduced from WINDII/UARS global measurements. *J. Geophys. Res.* **110**, A03304 (2005).
3. Witasse, O., Lilensten, J., Lathuillière, C. & Blelly, P. L. Modeling the OI 630.0 and 557.7 nm thermospheric dayglow during EISCAT-WINDII coordinated measurements. *J. Geophys. Res.* **104**, 24639–24655 (1999).
4. Fox, J. L. & Dalgarno, A. Ionization, luminosity, and heating of the upper atmosphere of Mars. *J. Geophys. Res.* **84**, 7315–7333 (1979).
5. Barth, C. A. The atmosphere of Mars. *Annu. Rev. Earth Planet. Sci.* **2**, 333–367 (1974).
6. Stewart, A. I. Mariner 6 and 7 ultraviolet spectrometer experiment: implications of CO_2^+, CO and O airglow. *J. Geophys. Res.* **77**, 54–68 (1972).
7. Leblanc, F., Chaufray, J. Y., Lilensten, J., Witasse, O. & Bertaux, J. L. Martian dayglow as seen by the SPICAM UV spectrograph on Mars Express. *J. Geophys. Res.* **111**, E09S11 (2006).
8. Jain, S. K. et al. The structure and variability of Mars upper atmosphere as seen in MAVEN/IUVS dayglow observations. *Geophys. Res. Lett.* **42**, 9023–9030 (2015).
9. Slanger, T. G., Cosby, P. C., Sharpee, B. D., Minschwaner, K. R. & Siskind, D. E. O(^{1}S→ ^{1}D, ^{3}P) branching ratio as measured in the terrestrial nightglow. *J. Geophys. Res.* **111**, A12318 (2006).
10. Gattinger, R. L. et al. Observation of the 557.7 nm to 297.2 nm brightness ratio in the auroral spectrum with OSIRIS on Odin. *Can. J. Phys.* **87**, 1133–1137 (2009).
11. Vandaele, A. C. et al. Science objectives and performances of NOMAD, a spectrometer suite for the ExoMars TGO mission. *Planet. Space Sci.* **119**, 233–249 (2018).
12. Vandaele, A. C. et al. Optical and radiometric models of the NOMAD instrument part I: the UVIS channel. *Opt. Express* **23**, 30028–30042 (2015).
13. Patel, M. R. et al. NOMAD spectrometer on the ExoMars trace gas orbiter mission: part 2—design, manufacturing, and testing of the ultraviolet and visible channel. *Appl. Opt.* **56**, 2771–2782 (2017).
14. López-Valverde, M. A. et al. Investigations of the Mars upper atmosphere with ExoMars Trace Gas Orbiter. *Space Sci. Rev.* **214**, 29 (2018).
15. Gkouvelis, L. et al. The O (^{1}S) 297.2-nm dayglow emission: a tracer of CO_2 density variations in the martian lower thermosphere. *J. Geophys. Res.* **123**, 3119–3132 (2018).
16. Gérard, J. C. et al. MAVEN IUVS observations of the CO_2^+ UV doublet and CO cameron bands in the martian thermosphere: aeronomy, seasonal and latitudinal distribution. *J. Geophys. Res.* **124**, 5816–5827 (2019).
17. Lawrence, G. M. Production of O(^{1}S) from photodissociation of CO_2. *J. Chem. Phys.* **57**, 5616–5617 (1972).
18. Gkouvelis, L. et al. Airglow remote sensing of the seasonal variation of the martian upper atmosphere: MAVEN limb observations and model comparison. *Icarus* **341**, 113666 (2020).
19. Forget, F. et al. Improved general circulation models of the Martian atmosphere from the surface to above 80 km. *J. Geophys. Res.* **104**, 24155–24175 (1999).
20. González-Galindo, F., López-Valverde, M. A., Angelat i Coll, M. & Forget, F. Extension of a Martian general circulation model to thermospheric altitudes: UV heating and photochemical models. *J. Geophys. Res.* **110**, E09008 (2005).
21. Thiemann, E. et al. The MAVEN EUVM model of solar spectral irradiance variability at Mars: algorithms and results. *J. Geophys. Res.* **122**, 2748–2767 (2017).
22. Chantler, C. T., Nguyen, T. V. B., Lowe, J. A. & Grant, I. P. Relativistic calculation of transition probabilities for 557.7 nm and 297.2 nm emission lines in oxygen. *Astrophys. J.* **769**, 84 (2013).

Acknowledgements

B.H. is research associate and S.A. is postdoctoral researcher of the Belgian Fund for Scientific Research (FNRS). ExoMars is a space mission of the ESA and Roscosmos. The NOMAD experiment is led by the IASB-BIRA, assisted by Co-PI teams from Spain (IAA-CSIC), Italy (INAF-IAPS) and the United Kingdom (The Open University). This project acknowledges funding from BELSPO, with the financial and contractual coordination by the ESA Prodex Office (PEA grant numbers 4000103401 and 4000121493). M.A.L.-V. and J.-J.L.-M. were supported by grant number PGC2018-101836-B-100 (MCIU/AEI/FEDER, EU) and by the Spanish Science Ministry Centro de Excelencia Severo Ochoa Program under grant number SEV-2017-0709. We also acknowledge support from the UK Space Agency through grant numbers ST/R005761/1, ST/P001262/1 and ST/S00145X/1 and the Italian Space Agency through grant number 2018-2-HH.0. We thank the ESA TGO team and its project scientist H. Svedhem for supporting observations in this special mode.

Author contributions

J.-C.G conceived the study together with L.G. and M.A.L.-V. and wrote the paper. S.A. analysed the data and Y.W., C.D., B.B. and I.R.T. calibrated the UVIS data and prepared the datasets. Observation planning was managed by B.R., M.R.P., J.-J.L.-M., J.M. and I.R.T. L.G. provided the 557.7 nm airglow model. A.C.V. is the NOMAD principal investigator and J.-J.L.-M., G.B. and M.R.P. are NOMAD co-principal investigators. F.D., B.H. and the other authors contributed to discussion and comments on the manuscript.

Competing interests

The authors declare no competing interests.

Additional information

Supplementary information is available for this paper at https://doi.org/10.1038/s41550-020-1123-2.

Correspondence and requests for materials should be addressed to J.-C.G.

Reprints and permissions information is available at www.nature.com/reprints.

Publisher's note Springer Nature remains neutral with regard to jurisdictional claims in published maps and institutional affiliations.